Alma Mater Studiorum - Università di Bologna

OCNUS

Quaderni della Scuola di Specializzazione
in Beni Archeologici

22
2014

ESTRATTI

Ante
Quem

Il logo di Ocnus si ispira a un bronzetto del VI sec. a.C. dalla fonderia lungo la plateia *A, Marzabotto (Museo Nazionale Etrusco "P. Aria", disegno di Giacomo Benati).*

Editore e abbonamenti
Ante Quem
Via Senzanome 10, 40123 Bologna
tel. e fax + 39 051 4211109
www.antequem.it

Abbonamento
□40,00

Sito web
www.ocnus.unibo.it

Richiesta di scambi
Biblioteca del Dipartimento di Storia Culture Civiltà
Piazza San Giovanni in Monte 2, 40124 Bologna
tel. +39 051 2097700; fax +39 051 2097802; antonella.tonelli@unibo.it

Le sigle utilizzate per i titoli dei periodici sono quelle indicate
nella «Archäologische Bibliographie» edita a cura
del Deutsches Archäologisches Institut.

Autorizzazione tribunale di Bologna nr. 6803 del 17.4.1988

ISSN 1122-6315
ISBN 978-88-7849-095-6

Indice

Recensioni

Five Centuries of Mosaic Glass at Saint Severus (Classe, Ravenna)

Mariangela Vandini[1], Rossella Arletti[2], Enrico Cirelli[3]

The basilica *and monastery of St. Severus are significant archaeological contexts for understanding how the monumentalization of Classe (Ravenna) proceeded since the 5th century AD. The archaeological campaign of 2011 in the area of the monastery – dated from the end of the 9th century – has brought to light several mosaic tesserae. In addition, recent restoration works carried out on mosaics discovered in the 1960s revealed some glass tesserae. These were sampled from two different mosaic floors removed from the St. Severus area: two floor fragments detached from the area of the so-called St. Rufillus's sanctuary (4th century), as well as from the northern aisle of the* basilica *(6th century). The latter is now located as a pastiche on the floor of an 18th century building in Ravenna (the so called Cripta Rasponi). Forty-one glass tesserae of different colours were analysed by means of EMPA-WDS, XRPD and SEM-EDS. The analyses aimed at identifying the raw materials employed in the mosaic glass production from the area of St. Severus, in order to compare the three sample sets and verify their chronology. Although the analysed tesserae revealed to be all of the natron type, a distinction among the different sample sets was clearly established on the basis of colorants and accessory components.*

Introduction

The site of Classe (Ravenna, Italy), nucleus of the Late Antique city, is currently subject to archaeological excavations by the University of Bologna, directed by Prof. A. Augenti (Augenti 2006a; 2006b; Augenti et al. 2006; 2012). The Basilica and the Monastery of Saint Severus, the religious centres of the area, are archaeological contexts of paramount importance for the study of the expansion of monumental buildings in Classe (Ravenna) starting from the 5th century AD (Cirelli 2014). The basilica of Saint Severus was first brought to light during an excavation campaign conducted by Giovanna Bermond Montanari in 1964 (Bermond Montanari 1966; 1968). More recent excavations, starting in 2006, have enabled a better definition of its profile, extending the archaeological investigations to a very large area occupied by a monastery built alongside the basilica at the end of the 9th century AD (Augenti 2010; Cirelli, Lo Mele 2010).

The site of Classe is divided into two separate sections, now representing two distinct archaeological areas a few kilometres apart, regarding the commercial and productive area of the town, and the religious area occupied by the Saint Severus basilica and monastery. The site is highly stratified due to its multifaceted history, strictly linked to that of the imperial town Ravenna (fig. 1 – for an exhaustive history of the site see Augenti 2011-2012).

The archaeological area of Saint Severus began to be occupied in the 1st century BC by a Roman villa whose planimetry is still not completely understood. It is certainly known that during the second half of the 4th century, before being included within the city walls of Classe, a new type of building was erected in the site of the villa: a *sacellum*, that Andrea Agnello's Liber Pontificalis testifies titled to St. Rufillo – a mausoleum dedicated to the owner of the ancient villa and hosted few decades later the remains of the bishop Severus (bishop in Ravenna during the 4th century AD). The actual change in the outline of the area occurred near the end of the 6th century, with the construction of a major basilica dedicated to Saint Severus whose completion and consecration took place in either 592 or 593 AD. A wider *sacellum*

[1] Department of Cultural Heritage - Alma Mater Studiorum University of Bologna (Ravenna branch), via degli Ariani 1, 48121 Ravenna, Italy.
[2] Department of Earth Sciences, University of Turin, via Valperga Caluso 35, 10125 Torino, Italy.
[3] Department of History and Culture, Alma Mater Studiorum University of Bologna (Ravenna branch), via San Vitale 28-30, 48121 Ravenna, Italy.

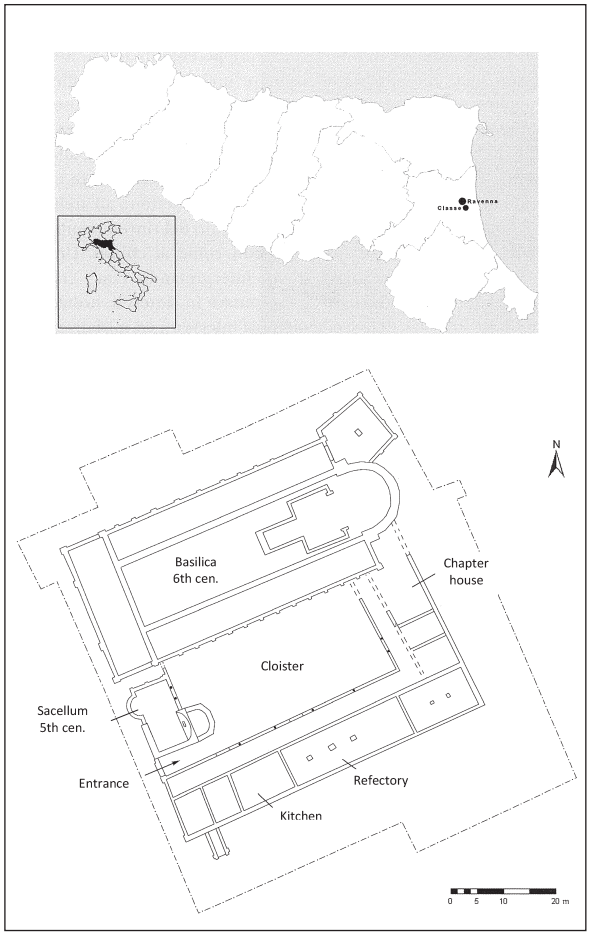

Fig. 1. Location of Classe and reconstruction of the St. Severus area (modified after Augenti 2011-2012)

was added in the same period with gorgeous polychrome mosaics (fig. 2) to host the Bishop's family and other élitarian burials, to the south side of the older building. Possibly, one of the first acts was to move the saint's body and relics in the basilica, the *sacellum* continued to be used as privileged shrine and selected burials zone still during the 9th century (Ferreri 2011). The 4th century mosaic pavement and the southern addiction were cut and restored many times, also trying to imitate the previous fine decoration, with clumsy results, as in the case of the end of the 8th century grave excavated in season 2013 (fig. 3). The end of the 6th century marks the beginning of the long life of the monumental area and especially of the basilica that, due to its religious importance, was preciously adorned with mosaics, fixtures and fittings of various kind. In the following centuries, maintenance work continued through time and possibly ended in the 15th century, when the ecclesiastical building was partially abandoned and the church was reduced at a single-nave church.

The Benedictine monastery of Saint Severus was firstly cited in written sources in the mid-10th century: archaeological data allow us anticipating its construction to the end of the 9th century, when it was erected along the southern wall of the basilica (Augenti 2011-2012; Augenti et al. 2012). With various phases and changes of destination of the buildings, the ecclesial complex went through important restoration works in the 13th and 15th centuries when the very bad state of conservation made it necessary to tear down parts of the basilica with the inevitable loss of the mosaic decorations. However, the monastery remained active until the year 1512, when the monks left the site. An attempt to restore the ruins was made around the mid 18th century, but with very poor results. The complete destruction of the basilica and the destruction and despoilment of the site finally took place in 1820 (Christie 2006).

During the recent excavation campaigns many glass finds were brought to light: glass vessels, lamps, mosaic tesserae, together with production markers (raw glass, semi-manufactured products, and glass waste) widely found both in the productive and commercial areas of Classe and close to the monastery, indicating the possible existence of glass workshops (Tontini 2006; Cirelli, Tontini 2010). In general, the glass finds, dated both on the basis of chrono-tipological criteria and stratigraphic location within the archaeological contexts, cover a wide chronological range, extending from the 4th to the 15th century AD.

The archaeological campaign of 2011 in the area of the monastery produced a collection of differently coloured mosaic tesserae. Most of the material is residual and cannot be precisely dated. In this work, a set of tesserae was studied from the area of the monastery originating from levels dated on the basis of stratigraphical position to the 9th to 10th century. The data relative to the tesserae from the monastery excavations (sample set SSV) have been already published (Fiori 2011; 2013). Nonetheless, the data are re-consi-dered: the samples not re-analyzed in view of the different approach of the present work, with the completely different aim of comparing the data to those from other new sets of mosaic tesserae, also considering updated and deeper archaeological information. In fact, in addition to the samples from the monastery excavations, some mosaic glass tesserae were sampled from two different recently restored mosaic floors – with the presence of a few glass tesserae among the stone ones – removed from the

Saint Severus area. One of the sample sets comes from a floor mosaic removed in the 1960s. This fragment comes from the zone of the so-called *sacellum*, the first nucleus of the Saint Severus area (second half of the 4th century) but its chronology is still a matter of controversy since it might be attributable to a 9th century remake. A second group of tesserae were sampled from some floor fragments (Foschini 2010) originating from the northern aisle of the basilica (6th century) and now located as a *pastiche* on the floor of an 18th century building in the centre of Ravenna (the so called *Cripta Rasponi*).

Overall, twenty three glass tesserae of different colours and degrees of opacity, originating from the excavation of the monastery (SSV, 9th -10th cen), were sampled and analysed, twelve tesserae from the floor of the *sacellum* (SAC, 4th cen), and six tesserae from the floor of *Cripta Rasponi* (CR, 6th cen, fragments detached from the floor of the Saint Severus basilica).

The aims of this work were: 1) to identify the raw materials, colourants, and opacifiers employed in mosaic glass production in the Saint Severus area; 2) to compare the three sample sets and verify their different chronology, when possible. This second aim would be an important goal, shared with the archaeological research: mosaic glass findings could be chronologically attributed only on the basis of their stratigraphic position since no typological criteria could be applied as for vessel glass. Furthermore, due to its fragmentary nature, mosaic glass could be easily re-employed and or/dispersed; therefore, the chemical-mineralogical results would be of archaeological significance. The results of this work are also important to deepen and widen knowledge of mosaic glass technology within the context of the abundance of mosaic glass in the town of Ravenna (Fiori et al. 2004; Vandini et al. 2006; Verità 2011), adding data regarding a period of time (9th century AD) with scarce comparison in the Mediterranean World.

Fig. 2. St. Severus 6th century mosaic floor from St. Rufillo shrine

Fig. 3. Mosaic epigraph from an 8th\9th century burial inside St. Rufillo shrine

Experimental

Electron Microprobe Analysis (EMPA)

The chemical analyses were carried out on polished samples using an ARL - SEMQ electron microprobe, equipped with four scanning wavelength spectrometers, sited at the Department of Earth Science of Modena and Reggio Emilia University. The elements analysed were: Si, Ti, Al, Mn, Mg, Fe, Ca, K, Na, P, Cl, S, Sn, Pb, Sb, Cu, Co, Cr. The following geological standards were employed: albite (Na); olivine (Mg); micro-

cline (K, Al); clinopyroxene (Si, Ca); sodalite (Cl), apatite (P); ilmenite (Fe, Ti); spessartine (Mn); chromite (Cr); cerussite (Pb). Metallic cobalt and metallic antimony were used for Co and Sb calibration, while synthetic cassiterite, $Cu_{94}Sn_6$ alloy and synthetic sulphide $Pb_4Ag_6Sb_6S_{16}$ were used for the calibration of Sn, Cu, and S, respectively. The analyses were performed operating at 15 kV, 20 nA, using counting times of 5, 10, 5 sec. on background-peak-background respectively. To prevent the known migration phenomenon of alkalis under the electron beam, a 30 μm defocused beam was used. On average, ten points were analysed on each sample to test homogeneity, and the mean value of all the measurements was calculated. The results were processed for matrix effects using the PHI(ρZ) absorption correction of the *Probe* program (Donovan and Rivers 1990).

The measuring accuracy for the analysed elements is better than 3%, with precision for major constituents between 1 and 2%, and minor constituents in the range of 2-3% (more details regarding the experimental procedure are reported in Arletti et al. 2011). The results of the chemical analyses expressed in weight% oxides are reported in tab. 1.

X-Ray Powder Diffraction (XRPD)

The X-ray diffraction experiments were performed on the opaque samples to identify crystalline phases dispersed in the glass matrix. The analyses were carried out with a diffractometer XPERT PRO PanAlytical with Bragg-Brentano geometry θ / θ and CuK_α radiation. The X-ray diffraction experiments were carried out following a non-destructive procedure, directly on the tesserae using an appropriate multi purpose sample stage to avoid physical sampling. The spectra were collected from 5 to 80 ° 2θ, using a 0.02 θ step and counting time of 4 sec. for each step. The results are reported in tab. 1.

Environmental Electron Scanning Microscopy (ESEM-EDS)

Backscattered electron images (BSE) and EDS spectra were collected on a low vacuum ESEM Quanta 200 – equipped with an Oxford energy dispersive spectrometer. Due to the low vacuum environment, all the analyses were performed directly on the tesserae, thereby avoiding sampling and carbon coating. The analyses were performed

LINE	Color	XRD	SiO_2	Al_2O_3	TiO_2	MnO	MgO	FeO	CaO	Na_2O	K_2O	Sb_2O_3	Cu_2O	PbO	SnO_2	CoO	SO_3	Cl	Cr_2O_3	P_2O_5	Totals
SSV1	light green	-	59,54	1,79	0,12	n.d.	0,74	0,43	5,88	18,00	0,35	n.d.	0,88	8,17	1,03	n.d.	0,30	1,12	n.d.	n.d.	98,44
SSV2	light green	no peaks	61,10	1,80	0,11	n.d.	0,80	0,47	6,30	18,28	0,35	0,02	0,85	6,43	0,75	n.d.	0,34	1,18	n.d.	0,05	98,87
SSV3	green	-	65,69	2,30	0,07	0,36	0,56	0,61	7,25	18,04	0,68	0,36	2,14	0,66	0,09	n.d.	0,20	1,17	0,03	0,18	100,37
SSV4	green	no peaks	60,37	1,71	0,11	0,06	0,71	0,50	5,44	16,99	0,30	0,02	1,12	9,04	1,44	n.d.	0,31	1,04	n.d.	0,05	99,21
SSV5	green	-	63,28	1,92	0,24	0,10	0,62	1,61	6,54	15,38	0,38	0,01	2,36	4,67	0,41	n.d.	0,23	1,03	n.d.	n.d.	98,81
SSV6	blue-green	-	61,95	1,86	0,12	0,03	0,73	0,58	5,63	18,47	0,33	0,03	1,18	6,59	0,92	n.d.	0,29	1,11	n.d.	n.d.	99,85
SSV7	blue-green	no peaks	65,55	2,25	0,10	0,69	0,54	0,54	6,35	17,25	0,76	0,79	2,34	1,57	0,12	n.d.	0,28	1,24	n.d.	0,12	100,51
SSV8	dark blue green	no peaks	64,80	2,26	0,11	0,54	0,54	0,54	5,81	17,21	0,75	1,12	4,36	0,50	0,21	n.d.	0,28	1,24	n.d.	0,07	100,36
SSV9	light blue (O)	$CaSb_2O_6$	64,59	2,31	0,11	0,71	0,60	0,41	8,08	14,98	0,70	4,85	0,17	0,14	0,02	n.d.	0,38	0,89	n.d.	0,16	99,12
SSV10	turquoise (O)	$CaSb_2O_6$	66,95	2,05	0,09	0,66	0,47	0,40	5,94	17,91	0,63	2,35	1,16	0,31	0,08	n.d.	0,33	0,81	n.d.	0,09	100,25
SSV11	turquoise (O)	$CaSb_2O_6$	66,95	2,25	0,08	0,66	0,53	0,40	6,50	16,14	0,71	2,35	2,51	0,46	0,31	n.d.	0,37	0,86	n.d.	0,11	101,18
SSV13	turquoise (O)	no peaks	67,05	2,13	0,13	0,18	0,78	0,47	4,56	19,79	0,56	1,57	2,39	0,20	0,13	n.d.	0,29	1,37	n.d.	0,08	101,67
SSV14	light blue (O) (purple nuance)	$Ca_2Sb_2O_7$	60,51	2,21	0,07	0,49	0,46	0,94	8,78	13,90	0,64	9,92	0,36	n.d.	n.d.	0,11	0,45	0,59	n.d.	0,09	99,52
SSV15a	colorless	-	70,39	2,54	0,16	n.d.	0,89	0,53	9,77	13,47	0,78	0,47	n.d.	n.d.	n.d.	n.d.	0,55	1,17	0,07	0,11	100,91
SSV15b	colorless	-	67,18	2,39	0,14	n.d.	0,84	0,57	9,25	15,59	0,86	0,40	n.d.	n.d.	n.d.	n.d.	0,41	1,14	n.d.	0,08	98,91
SSV16	colorless	-	70,35	1,99	0,10	0,08	0,47	0,31	6,07	17,70	0,54	0,89	0,07	0,12	n.d.	n.d.	0,30	1,45	n.d.	0,10	100,55
SSV17	colorless	-	68,97	2,04	0,08	0,30	0,44	0,27	5,42	20,53	0,51	0,58	n.d.	0,04	n.d.	n.d.	0,20	1,34	n.d.	0,07	100,84
SSV18	colorless	-	68,90	1,79	0,09	0,15	0,36	0,27	5,35	19,84	0,51	0,65	0,07	0,14	n.d.	0,03	0,24	1,40	n.d.	0,05	99,83
SSV19	colorless	-	64,44	2,31	0,13	n.d.	0,59	0,50	8,00	20,25	0,56	1,50	n.d.	0,06	n.d.	n.d.	0,32	1,55	n.d.	0,06	100,32
SSV20	colorless (green nuance)	-	66,26	2,11	0,11	1,32	0,56	0,50	6,75	18,11	0,48	0,03	n.d.	0,08	n.d.	n.d.	0,24	1,54	0,03	0,05	98,21
SSV21	red (O)	Cu^0	53,91	2,41	0,21	1,13	1,02	1,86	7,34	14,67	1,11	0,10	2,15	7,55	3,02	n.d.	0,29	0,85	n.d.	0,35	98,00
SSV22	brick red (O)	Cu^0	59,61	2,50	0,18	0,78	0,96	1,66	8,18	15,59	1,08	0,05	1,54	4,74	1,81	n.d.	0,32	0,98	n.d.	0,29	100,28
SSV23	brick red (O)	Cu^0	57,41	2,47	0,20	1,15	1,08	1,50	7,95	16,76	1,04	0,07	1,98	5,03	2,31	n.d.	0,30	0,91	n.d.	0,26	100,46
SAC1	white	-	67,36	1,92	0,10	0,08	0,62	0,42	5,88	19,19	0,48	0,79	n.d.	0,04	n.d.	n.d.	0,37	1,75	n.d.	n.d.	99,01
SAC2	colorless (grey nuance)	-	65,65	1,92	0,10	1,29	0,86	0,50	6,26	20,37	0,35	n.d.	n.d.	n.d.	n.d.	n.d.	0,27	2,08	n.d.	n.d.	99,70
SAC3	colorless (green nuance)	-	69,11	1,63	0,08	0,38	0,63	0,36	6,83	17,61	0,33	0,16	n.d.	n.d.	n.d.	n.d.	0,31	1,56	n.d.	n.d.	99,03
SAC4	colorless (green nuance)	-	64,39	2,09	0,29	2,17	1,00	0,99	5,68	20,66	0,34	n.d.	n.d.	n.d.	n.d.	n.d.	0,34	1,77	n.d.	n.d.	99,77
SAC5	colorless (weathered)	-	63,84	2,29	0,14	1,55	1,24	0,83	7,57	18,75	0,72	n.d.	n.d.	n.d.	n.d.	n.d.	0,42	1,33	n.d.	n.d.	98,75
SAC6	colorless (ocre nuance)	-	63,22	2,28	0,14	1,68	1,23	0,93	7,69	18,78	0,69	n.d.	n.d.	n.d.	n.d.	n.d.	0,42	1,34	n.d.	n.d.	98,46
SAC7	colorless (purple nuance)	-	66,38	1,92	0,10	1,73	0,77	0,60	7,15	18,55	0,60	n.d.	n.d.	n.d.	n.d.	n.d.	0,37	1,12	n.d.	n.d.	99,32
SAC8	light green	-	68,59	2,22	0,34	0,26	0,87	1,04	4,96	18,57	0,55	n.d.	n.d.	n.d.	n.d.	n.d.	0,32	1,44	n.d.	n.d.	99,22
SAC9	aqua green	-	67,49	2,30	0,39	0,24	0,90	1,07	4,88	18,13	0,43	n.d.	1,10	0,11	0,05	n.d.	0,32	1,46	n.d.	n.d.	98,87
SAC10	turquoise (O)	-	64,82	1,93	0,14	0,02	0,61	0,68	3,82	18,14	0,41	1,98	3,44	0,73	0,24	n.d.	0,30	1,59	n.d.	n.d.	98,86
SAC11	blue	-	68,86	1,67	0,08	0,59	0,47	0,74	6,17	17,90	0,49	n.d.	0,07	0,06	n.d.	0,05	0,27	1,45	n.d.	n.d.	98,90
SAC12	yellow (O)	-	49,72	1,78	0,13	1,41	1,00	0,69	6,31	14,19	0,56	n.d.	0,23	17,98	1,43	n.d.	0,31	0,91	n.d.	n.d.	96,66
CR1	blue	-	55,41	2,45	0,28	0,95	1,13	2,68	6,96	14,49	1,04	n.d.	1,66	7,27	2,91	n.d.	0,23	1,06	n.d.	0,23	98,79
CR2	blue	-	64,21	2,34	0,18	1,13	1,11	1,28	8,25	18,14	0,73	n.d.	0,12	0,50	0,06	0,10	0,34	1,12	n.d.	0,07	99,69
CR3	aqua green	-	66,08	2,07	0,15	0,05	0,92	0,67	7,17	19,99	0,37	n.d.	1,05	0,04	0,02	n.d.	0,36	1,75	n.d.	n.d.	100,73
CR4	turquoise (O)	-	66,17	1,73	0,08	0,01	0,45	0,41	5,41	16,79	0,57	1,54	3,30	1,34	0,27	n.d.	0,26	1,45	n.d.	n.d.	99,82
CR5A	red (O)	-	66,25	1,77	0,07	0,02	0,46	0,41	5,37	17,01	0,52	1,44	3,19	1,34	0,22	n.d.	0,30	1,45	n.d.	n.d.	99,84
CR5B	blue	-	64,48	2,36	0,16	1,15	1,14	1,29	8,31	18,04	0,74	n.d.	0,10	0,45	0,02	0,10	0,31	1,11	n.d.	0,10	99,91

Tab. 1. Chemical analyses (oxides wt%) obtained by EMPA for the analysed samples. (Abbreviation: (O)= opaque; nd. = not detected)

using an acceleration voltage of 25 kV and a working distance of 13 mm. The BSE images were mainly collected on opaque glasses to evidence the presence of crystalline opacifying agents in the glass matrix and define their morphology, and EDS analyses were run to obtain qualitative chemical analysis on these inclusions.

Results

Chemical composition

The chemical compositions of major and minor elements of the three sample sets are reported in tab. 1. All the analyzed samples are silica soda glass containing SiO_2 ranging from 49.72 wt.% to 70.39 wt.%, Na_2O from 13.47 wt.% to 20.66 wt.%, and CaO from 3.82 wt.% to 9.77 wt.%. The low levels of MgO and K_2O reported in fig. 4 clearly indicated that all the samples were produced using an inorganic source of alkalis, that is natron. From fig. 5, where the contents of Al_2O_3 and CaO are plotted, it is possible to hypothesize the use of a siliceous calcareous sand as vitrifying agent, with a feldspatic component. On average, the data reported in fig. 4 and 5 reveal typical Mediterranean Roman-Late Antique compositions for the three sample sets. However, it is possible to distinguish the sample sets on the basis of the relative differences in the amounts of the main oxides that allow a possible clustering. Some samples are characterized by high Al_2O_3, CaO and K_2O: nine SSV samples (SSV3, SSV9, SSV14, SSV15A, SSV15B, SSV19, SSV21, SSV22 and SSV23), three sample from *Cripta Rasponi* (CR1, CR2 and CR5B) and two samples from the sacellum (SAC5 and SAC6). On average, seven samples from the *sacellum* (SAC1, 2, 3, 7, 10, 11, 12) exhibit lower K_2O, CaO and Al_2O_3 and form an homogeneous group; among the remaining SAC tesserae, samples SAC5 and SAC6 contain higher MgO and rather high CaO with respect to the other SAC samples, where as SAC4, SAC8, SAC9 contain slightly higher Al_2O_3. An analogous subdivision in a more homogeneous group (with lower K_2O, MgO, CaO and Al_2O_3) can be found for the SSV set, in which samples SSV3, 9, 14, 15a, 15b, 19,21, 22, 23 are characterized by sensibly higher K_2O, MgO, CaO and Al_2O_3 with respect to the other SSV samples. The six samples from *Cripta Rasponi* split exactly into two groups: CR1, 2 and 5B with higher K_2O, MgO, CaO and Al_2O_3 and CR3, 4, 5A with lower contents of the same oxides. On the basis of the FeO and TiO_2 percentages (fig. 6), it is possible to observe some differences in the analyzed glass. Most of the samples from the three different groups exhibit TiO_2 lower than 0.2 wt. % and FeO lower than 1.0, values always referable to impurities deriving from minerals present in the sands used as vitrifying agent. Four samples from the SSV set (SSV21, 22, 23 and SSV5) and three

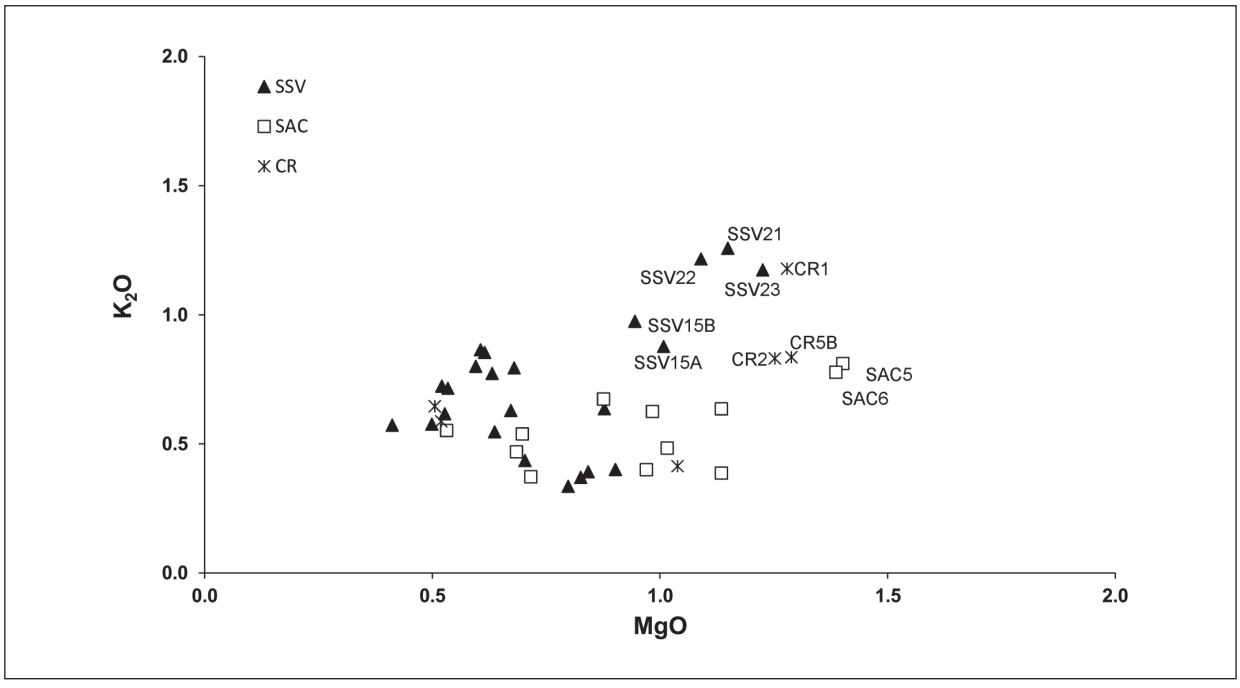

Fig. 4. Recalculated levels of K_2O vs. MgO contents for all the analysed samples

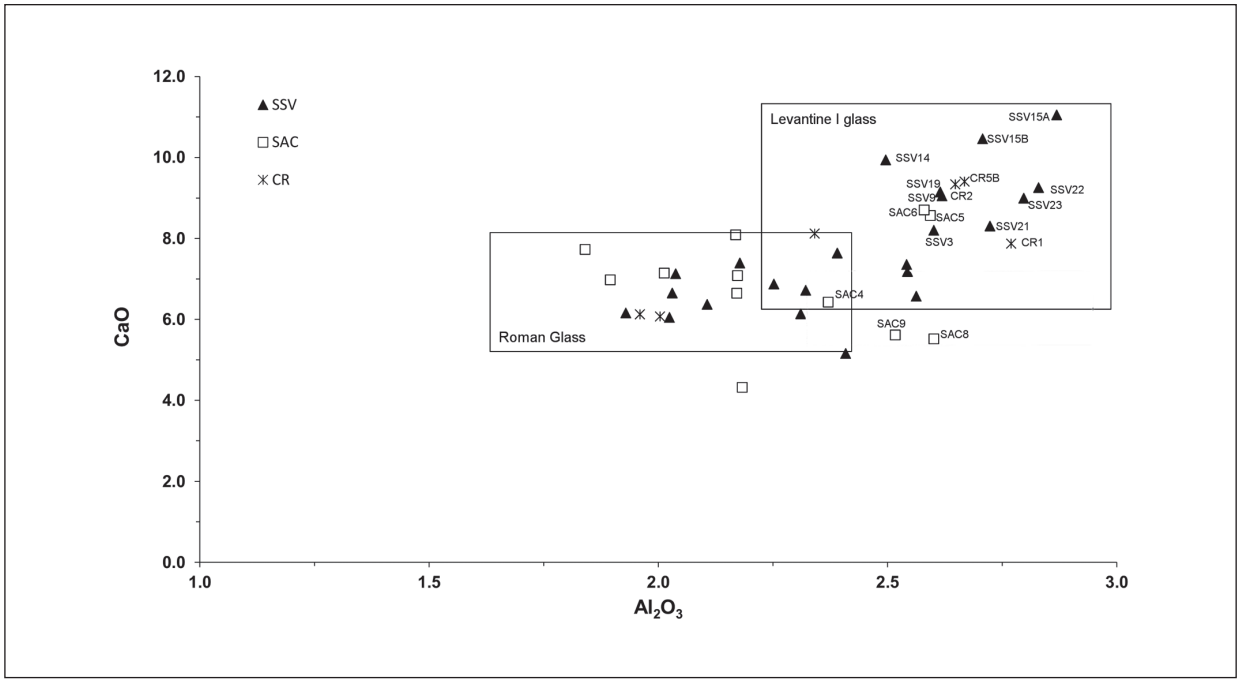

Fig. 5. Recalculated levels of CaO vs. Al_2O_3 contents for all the analysed samples. Square areas: field of the main natron glass compositional groups identified in literature (Nenna 2000; Freestone et al. 2000)

samples coming from the CR floor mosaic (CR1, CR2, and CR5B) – show higher and correlated values of FeO and TiO_2. These data, suggest that, being these samples deeply coloured, the high levels of iron should be related to the coloring elements rather than to the sands employed for glass production. Six of these seven samples have been already noted to be slight different from the others also regarding the main components. High values of TiO_2 and rather high values of FeO are also found on the three samples from the SAC set (the colourless SAC4, the light green SAC8, and the aqua green SAC9). This could be related to the presence of impurities present in the sand used as vitrifying, thus indicating the use of a different raw material for these tesserae, even if, regarding the major components, these samples fit perfectly with the main group to which they belong.

Manganese oxides are very heterogeneously distributed among the samples sets (fig. 7). The highest values are from the single yellow (SAC12) and five colourless SAC tesserae (all the colourless SAC tesserae with the exclusion of SAC1 and SAC3, have high MnO and negligible Sb_2O_3, see below). High manganese levels (higher than 1%) are found in three tesserae from SSV (two red - SSV21 and 23 - and one colourless tesserae SSV20) and two tesserae from the CR set (CR2 and CR5B blue).

The levels of colouring elements and the elements usually responsible for opacity are very heterogeneously distributed across the three sample sets. To emphasise the differences it is useful to consider the samples on the basis of their colour.

Blue and turquoise tesserae

Antimony oxide is present in amounts higher than 1% in all the turquoise and light blue opaque samples from all the sample sets. Basically, all the turquoise and light blue samples are coloured with copper, the oxide of this element being present at levels higher than 1%, and so intentionally added. The dark blue samples owe their colour to the presence of cobalt. Sample SSV9, contains very low Cu and Co, and therefore its colour is probably due to the iron present in the batch and perhaps to a very low content of cobalt (possibly very close to the detection limit of EMPA). The composition of the turquoise and light blue tesserae is very similar for the three sets with the sole exception of sample CR4 in which PbO slightly exceeds 1%. In all the blue samples PbO never exceeds 0.7% with the exclusion of CR1 in which a relatively high content of lead (PbO 7.27%) is accompanied by a quite high SnO_2 (2.91%).

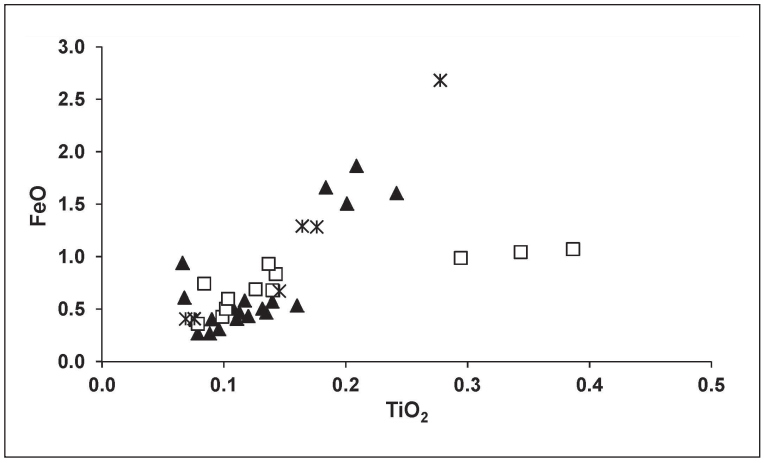

Fig. 6. Plot of FeO vs. TiO_2 contents for all the analysed samples

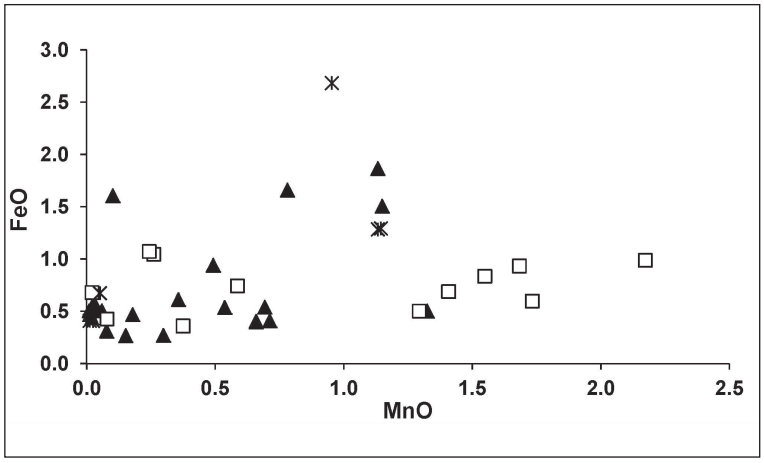

Fig. 7. Plot of FeO vs. MnO contents for all the analysed samples

Green tesserae

All the green tesserae appear transparent; SSV4, with the highest PbO and SnO_2 contents, shows a slight milky appearance. The green tesserae from SSV contain lead (even if in two cases, SSV3-8 there is less than 1% of PbO) and detectable amounts of SnO_2 while these two oxides are negligible in the green tesserae of the other two sample sets. It is worth noting that the green tesserae from the monastery excavations split into two groups as regards the contents of PbO and SnO_2 (low: SSV3, 7, 8; high: SSV1, 2, 4, 5, 6, with PbO/SnO_2 ratio from ~7 to ~ 11). A peculiarity is the tesserae SSV8, the only green containing antimony, low SnO_2 and a very high level of copper. The colour of all the green samples is the result of the addition of copper bearing minerals (the highest value of Cu_2O in measured in sample SSV8, the tessera showing the darkest nuance), with the exclusion of sample SAC8 whose iron level can be assumed to produce its very light green colour.

Colourless tesserae

There are no colourless tesserae in the CR sample set. The samples from to the other two groups exhibit different features: samples from SSV contain high antimony and no manganese (with only one exception - SSV20 - containing MnO and no Sb_2O_3). Samples SSV15a, b and 19 form a subgroup with high Ca and Al (fig. 5): they are the only three colourless glasses with no detectable manganese. Samples from the *sacellum* SAC contain only high manganese and no antimony the exception of SAC3 with low contents of both these oxides. In all these tesserae Pb, Sn, Cu, and Co are not detectable or negligible.

Red tesserae

Only four red tesserae were analysed, three from the excavation SSV sample set and one from the CR floor mosaic. The tesserae from the former contain high Cu_2O accompanied by high PbO, FeO, SnO_2, and quite high MnO and P_2O_5. In addition, these samples exhibit higher K_2O, MgO and TiO_2 with respect to the other samples, and slightly lower Na_2O. The red tessera of the CR set has high Cu_2O, PbO, and Sb_2O_3 but, is characterised by low levels of FeO, SnO_2, and not particularly high contents of K_2O, MgO and P_2O_5. It is worth noting that the chemical composition of the two samples CR4 turquoise and CR5A red are almost identical, proving that different colours were obtained by controlling the redox conditions.

White tessera

Only one whitish tesserae coming from the *sacellum* was analysed; it shows relatively high content of antimony, no tin and negligible lead.

Yellow tessera

Only one yellow tessera was analysed, from the *sacellum*. It contains very high lead (around 18 wt. % PbO) quite high tin oxide and manganese, and no detectable antimony.

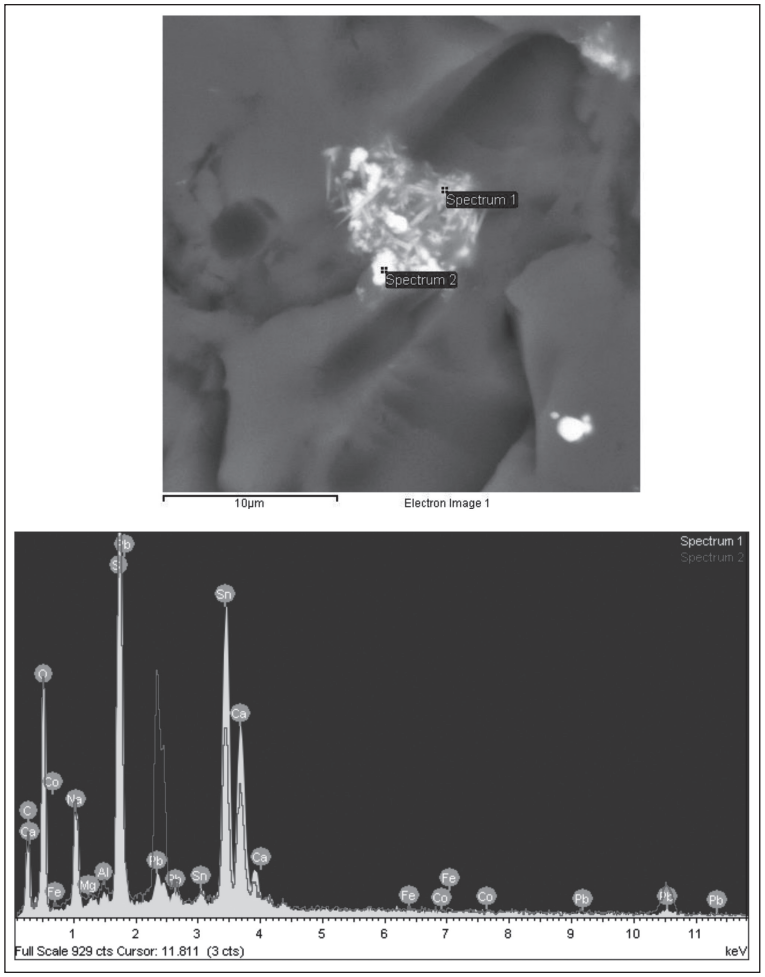

Fig. 8. BSE image and relative EDS spectra collected on sample SSV6 showing lead stannate and cassiterite crystals

X-ray diffraction analyses

X ray powder diffraction analyses were performed only on the samples from the SSV sample set due to unavailability of samples from the other two sets. The only phases detected in the samples were: calcium antimoniates, with two different structures ($CaSb_2O_6$ and $Ca_2Sb_2O_7$) in the turquoise and light blue samples (SSV9-10-11-14), and metallic copper in all the red samples. It is not possible to exclude the presence of crystalline phases in the other tesserae, since, if present in low quantities and/or small crystals, they would not have been detected with conventional X-ray diffraction measurements.

ESEM-EDS investigations

Scanning electron microscopy studies were performed only on selected samples from the monastery excavations, in particular on the blue, green, and red nuances. Some of the results are reported in figs. 8-11.

The green samples can be divided into two groups: samples SSV3-7-8 which do not contain inclusions, and samples SSV1-2-4-5-6 which contain particles with higher atomic number

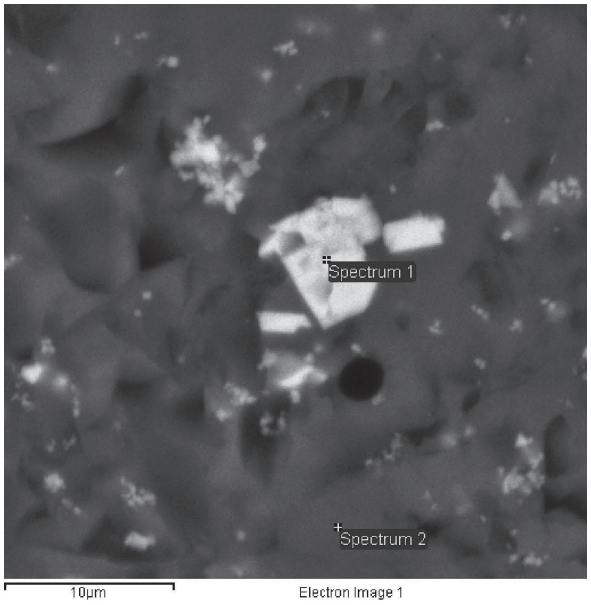

Fig. 9. BSE image collected on sample SSV10 showing prismatic crystals of calcium antimoniate

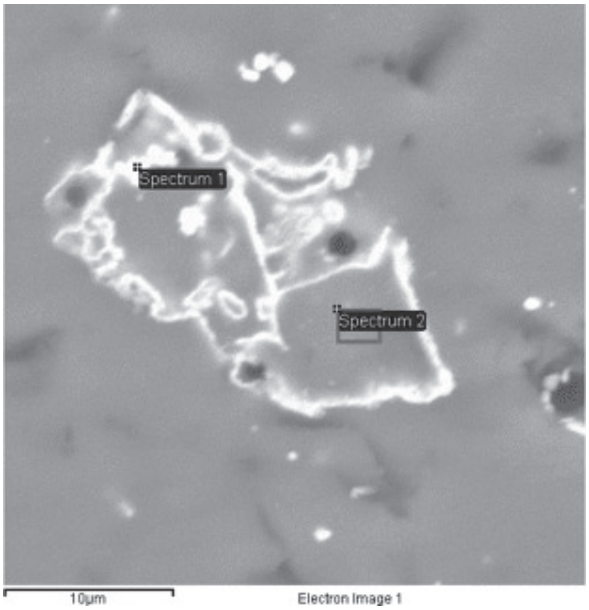

Fig. 10. BSE image collected on sample SSV9 show rosary shaped aggregates of calcium antimoniate crystals

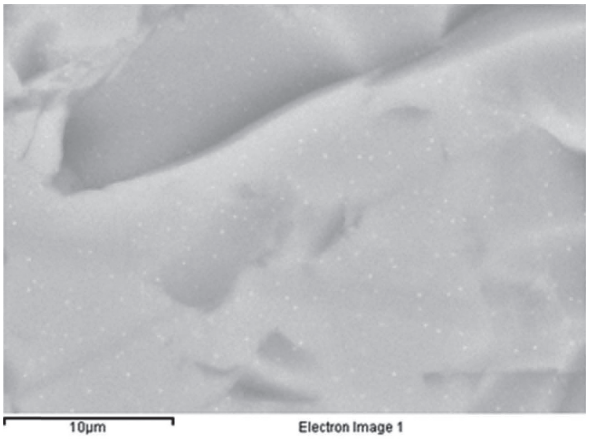

Fig. 11. BSE image collected on sample SSV22 showing CuO clusters

than the glass matrix. fig. 8 shows an example of the BSE image and relative EDS spectra collected on sample SSV6. In the image it is possible to distinguish two different kinds of particle exhibiting different morphology and a different contrast level. Very light grey spheroid particles are visible as well as slightly darker acicular crystals. The EDS spectra collected on both the typologies provided an explanation for the differing contrast found in the BSE image: the acicular crystals consist basically of Sn and oxygen (spectrum 1), while the spherical particles turn out to be Pb and Sn bearing particles (spectrum 2). The EDS spectrum on the matrix (not reported) shows that lead was also dispersed in the glass. This situation (presence of crystals of these two morphologies with different chemistry dispersed in a lead bearing matrix) is attested in all the Pb-Sn bearing green glass (SSV1-2-4-5-6), although XRPD analyses could not detect crystalline phases.

All the blue and turquoise samples reveal the presence of dispersed particles with higher atomic numbers. The EDS spectra allow the identification of calcium antimonates, very common opacifiers employed in the opaque glass of this period. In most cases (samples SSV10-11-13-14) the particles observed are well formed crystals, sometimes with prismatic habit of tens of microns, sometimes forming small aggregates (fig. 9). By contrast, in sample SSV9 the particles exhibit a different microstructure consisting of small crystals forming aggregates of rosary shapes, as reported in fig. 10.

The three red samples present a very common situation, typically found in red tesserae of this period. As shown in fig. 11 (image from SSV22) all the red opaque glass exhibits nanometric clusters of metallic copper, easily recognizable on the basis of shape. In addition, quite large aggregates of metallic tin (tens of micron), probably representing residues of the raw materials, were found dispersed in the glass matrix.

Discussion

As regards the main glass constituent, the tesserae here analysed are the typical soda-lime glass of natron type obtained using siliceous sands – with feldspatic components and calcareous fragments – and natron as a source of flux (the mineral trona, a salt derived from the Egyptian evaporitic deposits of Wadi-Natrûn mostly in the form of sodium sesquicarbonate e trisodium hydrogendicarbonate). This is a typical feature of mosaic glass produced in Roman and Byzantine times[1]. In particular, as regards the base raw materials, a very good comparison can be found with the glass tesserae from the basilica of Saint Vitale (Fiori et al. 2004) and Neoniano Baptistery, coming from mosaics located within a few kilometres distance from Classe: natron glass is the base constituent of all the original tesserae and the ranges of CaO and Al_2O_3 as indicative of the vitrifying raw material are perfectly overlapped.

The composition of the tesserae is quite homogeneous (a few exceptions will be discussed later on) and the occurrence of natron type glass suggests that all the tesserae possibly result from pre-10th century AD production, therefore solving the problem of dating the tesserae only on the basis of their stratigraphical position. At the end of the first millennium AD several changes occurred in glass manufacturing processes. During this period, and particularly between the 9th and 11th century, natron glass production started to be replaced and halophytic plant ashes began to be used as a fluxing agent for glass production together with purer sources of silica (Lilyquist, Brill 1993). The changeover was not abrupt but progressed leading to an intermediate stage with the appearance of the so called "mixed natron-plant ash composition" identified at Middle Eastern (Henderson et al. 2004) and Italian sites (Uboldi,

[1] Freestone et al. 1988; Fiori et al. 2004; Arletti et al. 2006; Vandini et al. 2006; Van der Werf et al. 2009; Verità, Santopadre 2009; Arletti et al. 2010; Silvestri et al. 2011; Verità 2011; Gliozzo et al. 2012; Schibille et al. 2012; Di Bella et al. 2014; Silvestri et al. 2014.

Verità 2003). Mosaic glass started to follow this trend during the 10th and 11th centuries and mixed compositions were identified in the Torcello Basilica (Andrescu-Treadgold, Henderson 2006) and the two Greek monasteries of Daphni and Hosios Loukas (Arletti et al. 2010). The tesserae sample set from the Saint Severus excavations do not belong to this transition phase, therefore it is reasonable to suppose that they were not produced after the 10th-11th century AD. Furthermore, both for the flux and vitrifying raw materials, close similarities can be observed with mosaic tesserae from the basilica of Santa Cecilia in Rome, dated at the 9th century AD (Verità, Santopadre 2009).

The recalculated composition (normalized to 100wt.% after the removal of the elements intentionally added as colorants or to confer opacity to the glass form the chemical data) is compared, with the compositional field of Roman and late antique transparent glass found in literature (Freestone et al. 2000; Nenna et al. 2000; Foy et al. 2003; Silvestri et al. 2008; Foster, Jackson 2009; Silvestri et al. 2011) (figs. 4-5) Although minor differences can be observed in the contents of K_2O and MgO, all samples fall in the field of natron glass. With the aim of a more general classification and comparison with coeval Mediterranean glass production, some differences can be found observing the CaO and Al_2O_3 levels. Most of the samples from the monastery excavations (SSV set) and from the sacellum (SAC set) fall inside the field characteristic of Roman glass, in which is also included half of the samples from *Cripta Rasponi* (CR set). The remaining samples of the SSV and CR sets and belong to the Levantine I group, which also contains three samples from the *sacellum*. The same subdivision between the Roman and Levantine I group is reported for the tesserae from Saint Vitale in Ravenna (Fiori et al. 2004).

The distinction made on the basis of the vitrifying base materials could lead to the suggestion of the use of different sands and the following peculiarities would support the hypothesis of a different production, chronologically attested after that of the typical Roman glass (possibly if the Levantine I type):

SSV set: the green samples with low Pb and Sn (differing form the other green tesseare of the same group – see below); the two light blue samples and the three colourless tesserae in which manganese is not detected ; finally, the three red samples whose characteristics are diffusely discussed below.

SAC set: two colourless samples SAC5 and 6 fall distinctively in the Levantine I group, and other three samples (SAC4, 8 and 9) are characterized by higher Al_2O_3; all these samples show higher FeO and MgO content.

CR set: the three blue tesserae, also showing higher K_2O and MgO.

The levels of FeO and TiO_2 shown in fig. 6 indicate that seven samples (four samples from SSV set – SSV21-22-23 and SSV5 – and three samples from CR floor mosaic – CR1, CR2, and CR5B) show high and correlated levels of the two elements. This, along with the high levels of MnO found in all these tesserae, seems to suggest that these samples could be classified as HIMT glass, however, this is definitely not the case for the red samples from the SSV set (see discussion below) for which the high content of these oxides could be related to deliberate additions to obtain the desired colours. The reason of the high levels of TiO_2 for sample SAC 4, SAC 8 and SAC 9 should be different, in fact these sample do not show high FeO and the content of MnO is relevant only in sample SAC 4 – but this is related to its colourless appearance (addition of manganese as decolouring agent) rather than to the sands employed for its production.

Many differences in the tesserae composition are related to the technique and the materials used for their opacification and coloration.

An homogenous situation is found for the turquoise and light blue opaque samples: all these samples were opacified with calcium antimonates, and contain lead in variable amounts, at most just above 1 wt% of PbO. The presence of copper and antimony (and traces of lead) is characteristic of a long time production of this nuance: from Roman (see e.g. Van der Werf et al. 2009 for Italian production; Paynter, Kearns 2011 for British findings) through Byzantine times (Fiori et al. 2004; Schibille et al. 2012).

As discussed in the previous section, the calcium antimonate found in these samples show, in most of the cases, well formed prismatic crystals and, in only one case (SSV 9) a more complex microstructure with small crystals forming aggregates of rosary shapes. A similar situation is discussed in the paper by Lahill et al. (2010) in which the nature of the Sb-bearing opacifiers has been deeply investigated. The authors suggested that the shape of the crystals of calcium antimonate inside the glass matrix could give indications regarding the technique employed for the opacification. In fact, they indicated the presence of submicronic crystals of Ca-antimonate organized in compact rosary shapes as the proof of an *ex situ* crystallization of the opacifier (ad-

dition of Ca-antimonate to the glass batch). On the contrary, the presence of Ca-antimonate polygonal crystals with average sizes greater than 1 μm is the indication of the *in situ* crystallization, obtained by adding Sb to a Ca-bearing glass (Shortland 2002). While the insertion of an antimony bearing raw material for the opacification of glass would not result in an increase of Ca oxide in the chemical analyses of the glass (being calcium already drawn out of the matrix), the addition of calcium antimonate to a Ca-bearing glass would lead to an increase of CaO in the bulk chemical analysis. This is consistent with our data, in fact, the tessera showing rosary shape antimonate – indication of *ex situ* crystallization of Ca-antimonates, thus the addition of Ca – is the sample with the higher CaO contents.

Calcium antimonate opacifiers are present in two different stoichiometry in the analyzed samples: in its hexagonal form ($CaSb_2O_6$) in samples SSV9, SSV10, SSV11, and in its orthorhombic one in sample SSV14. The reason of the presence of the two different phases should be found in the different kinetics and temperature of production of these tesserae. In fact, an experiment performed by Lahill et al. 2010 suggests that *in situ* crystallization of calcium antimonate after the addition of Sb_3O_4 lead to the formation of $CaSb_2O_6$ when heated for 2 days at 1100°. On the contrary, if the batch is heated for longer time (up to 13 days) the thermodynamically stable phase is $Ca_2Sb_2O_7$. The presence of the orthorhombic phase only, in sample SSV14, indicate that probably the firing of this glass lasted for more than two days, contrarily to samples SSV9, SSV10 and SSV12 probably heater for shorter time.

The dark blue sample does not contain antimonates and the final effect (hindering the transmission of light) is due to the presence of cobalt, associated to high amount of iron resulting in the deep colour. Blue mosaic glasses with Co as chromophore were extensively produced from Roman to later times, as cobalt blue tesserae could be still found in 9th century mosaic in Santa Cecilia, Rome (Verità, Santopadre 2009) and 10th-11th century tesserae from Torcello (Andrescu, Henderson 2006), Daphni and Hosios Loukas (Arletti et al. 2010). Only one sample from *Cripta Rasponi* (CR1) shows a different chemical composition (containing high tin and lead and being coloured with copper). One of the blue tesserae (CR1) is definitely distinguishable for its high lead, tin, and iron content (it could possibly be of non-6th century production), on the contrary CR2 and CR5B have a very similar composition, probably indicating they derive from the same glass chunk.

Out of ten green tesserare analysed, eight come from the monastery excavations (SSV). The green tesserae can be divided into two groups based on the contents of PbO and SnO_2 (low: SSV3, SSV7, SSV8, SAC 8, SAC9 and CR3; high: SSV1, 2, 4, 5, 6). The main chromophore is copper in both groups although a difference in its introduction can be recognised: in the low Pb – low Sn samples no crystalline inclusions can be singled out by SEM-EDS and there is no correlation between copper and tin (fig. 12), testifying the addition of "pure" copper. On the contrary, although the high Pb – high Sn green samples appear translucent, the SEM images show the presence of some particles dispersed in the matrix. Nevertheless the XRD analyses could not reveal the presence of crystalline particles in the samples: this could indicate that, even if some crystals

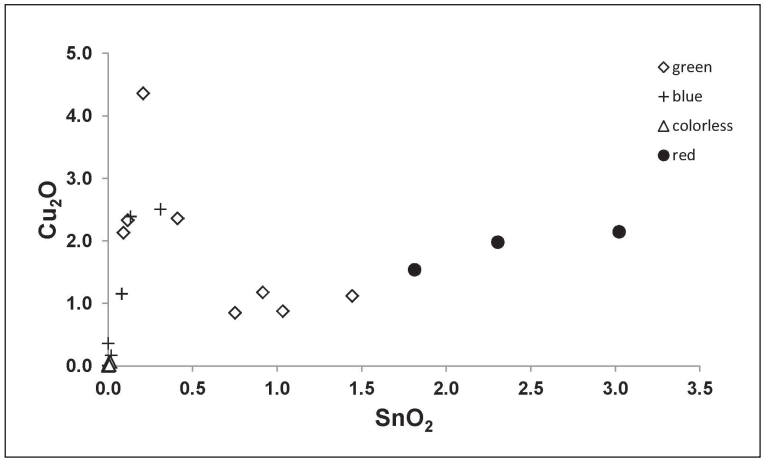

Fig. 12. Plot of Cu_2O vs. SnO_2 contents for all the analysed samples

are dispersed in the glass, their amount is too low to be detected by XRD and, as a consequence to impart an opaque effect. The presence of high and correlated amounts of PbO and SnO_2 could indicate the tentative addition of Pb, Sn- based opacifiers, typically employed in this period. In a recent work, Tite and colleagues (Tite et al., 2008) examined tin-opacified glass and proposed a reassessment of the method by which these materials may have been produced. They demonstrated that in a mixture of SiO_2, PbO, and SnO_2 the persistence of $PbSnO_3$ is favoured by low PbO/SnO_2

ratios and low levels of silica; otherwise the cubic lead stannate, responsible for the yellow colour, would be transformed into cassiterite at relatively low temperatures (around 750–850°C), preventing the formation of the desired shade. In the case of the green tesserae from Saint Severus, the high PbO/SnO_2 ratio and the high contents of silica, would lead to a very easy conversion of lead stannate to cassiterite. The presence of only few crystals of opacifiers and the co-presence of lead stannate and cassiterite crystals (as evidenced by SEM-EDS investigations) could be explained as partial decomposition of the lead stannate. However, this would have led to the crystallization of an higher amount of cassiterite.

An analogous relation between tin and lead can be recognised in all the red tesserae, in which the colour is due to the presence of copper in the reduced state; they also contain high iron and variable amounts of lead and tin; the red sample from *Cripta Rasponi* – CR set – shows a quite remarkable content of antimony. Although the cromophore is clearly the same, the red samples coming of the monastery excavation – SSV set – are different from that found in the *Cripta Rasponi* – CR set. In fact, while this latter shows K_2O and MgO levels compatible with all the other samples, the ones from the monastery are characterised by relatively higher levels of these elements, although well below the contents undoubtedly connected with the use of plant ash (Lilyquist, Brill 1993). When considering the red tesserae of the SSV set (SSV21 to 23) the higher contents of alkalis could be the evidence of the addition of small quantities of vegetal fuel ash (wood ash) in the melt to obtain reducing conditions. This is further supported by the presence of a higher phosphorous content, not detectable or in very low amounts in the rest of the sample set. The use of wood ash - and not plant ash - in the glass mix is testified by the lower content of Na and Cl: the addition of fuel ash would facilitate the reduction of cupric oxide to metallic copper – detected by XRPD (tab. 1) – as reported by other authors (Schibille et al. 2012) due to its reducing capacity (Cable, Smedley 1987; Freestone 1987; Paynter 2008). The reducing action is further guarantee by iron in the batch[2] as demonstrated by the highest content of FeO within the SSV red samples. The composition of the red tesserae from the monastery are clearly distinctive from the other tesserae of the same set, in agreement with the data reported in literature for Roman and Byzantine opaque red glass[3] but the same is not true for the red tesserae in the CR set, in which also the content of lead, tin and antimony make its composition clearly distinguishable from the SSV reds.

Previous studies on opaque red glass (Stapleton et al. 1999; Freestone et al. 2003; 2008; Barber et al. 2009), indicate the use of copper-lead-silica silver-refining slag, or its associated litharge for the copper reduction process. In the red mosaic glasses from Saint Severus monastery excavation copper contents are strongly correlated with tin (fig. 12), with the same ratio as found in the tin bearing green tesserae. This fact suggests that the raw materials employed to introduce copper and tin could the same, probably slags of metallurgical production (the Sn/Cu ration does not correspond to that of bronze), and that the different colours could be due to different redox conditions. In the SSV high Pb – high Sn green samples and in the red tesserae, tin is introduced as a contaminant of copper, possibly indicating the use of tin-rich debris (Freestone et al., 2003) or even possibly tin and lead metallurgical wastes since also a correlation between lead and tin can be recognized, recalling the use of lead debris to favour reducing conditions and the formation of metallic copper. The correlation SnO_2 vs. PbO – with Pb:Sn about 2:1 (matching that of pewter) – could indicate the use of an alloy (Fiori 2011).

As regards the copper rich red tesserae from the Saint Severus monastery, the use of fuel ash, the presence of copper related lead and tin are features recognizable in the Byzantine production although they cannot be considered an unique chronological signature (very low tin is reported by Shugar 2000; Arletti et al. 2010; Verità, Santopadre 2009); however, these red tesserae could be hardly considered as a re-use of Roman glass since, although compatible with the use of fuel ash, they are clearly distinguishable for low lead and especially tin content[4]. The high content of tin oxide in green and red samples from the monastery excavations allows to definitely exclude a Roman production and re-use of these tesserae: the use of

[2] Freestone 1987; Brill, Cahill 1988; Arletti et al. 2006; Van der Werf et al. 2009; Schibille et al. 2012.

[3] Cable, Smedley 1987; Freestone 1987; Brill, Cahill 1988; Freestone et al. 1990; Shugar 2000; Freestone et al. 2003; Barber et al. 2009; Van der Werf et al. 2009; Schibille et al. 2012; Silvestri et al. 2014.

[4] Santagostino Barbone et al. 2008; Paynter, Kearns 2011; Gliozzo et al. 2012; Di Bella et al. 2014.

tin in glass is considered a post-4th century introduction (Turner, Rooksby 1959; Tite et al. 2008) when it began to replace the Sb-based opacifiers, although its presence as an opacifier appeared as early as the 2nd century BC (Henderson 2000). The use of tin is attributed to late-antique productions (Verità et al. 2002; Santagostino Barbone et al. 2008) and used in Italy from the 5th century onwards (see e.g. Uboldi, Verità 2003; Fiori et al. 2004), eventually (7th-13th century) evolved in the technology of lead-tin calcine (Tite et al. 2008). It is worth noting that the yellow tessera in the SAC sample set shows high lead and tin content: if its production would be definitely proved coeval with the *sacellum* construction (second half of the 4th century), the use of tin in lead-tin opacified glass in Italy could be slightly anticipated.

On the contrary, the red sample CR5A is characterised by high copper, very low SnO_2 and relatively high Sb_2O_3: the lack of tin oxide was found by Shugar (2000) in Byzantine red tesserae from Israel and late Byzantine red tesserae from Daphni and Hosios Loukas (Arletti et al. 2010), but the presence of antimony in high amounts is not reported in the above cited literature on opaque red tesserae. Quite high antimony – even if about half of the quantity of Sb_2O_3 found in sample CR5A – is reported in a red tesserae from the 9th-10th century mosaic in St. Cecilia, Rome (Verità, Santopadre 2009), none or very low antimony (Sb_2O_3< 0.25 wt%) was found in the original red tesserae from Byzantine St. Vitale, Ravenna (Fiori et al. 2004) and St. Prosdocimus, Padua (Silvestri et al. 2013) or Roman Herculaneum (Van der Werf et al. 2009), making the red tesserae from *Cripta Rasponi* an exception. A possible hypothesis is that the red sample was possibly intended to be turquoise: its composition is almost identical to that of the turquoise sample CR4 and only the different furnace atmosphere could have determined the final colour.

Seven colourless tesserae were analysed from the Monastery excavations and six from the sacellum; no colourless tesserae was found in the *Cripta Rasponi* group.

The colourless tesserae usually represent the base of the metal leaf tesserae (mainly gold but sometimes also silver) made of a thin metal layer between a glass support (a few mm thick) and the cartellina, a thin (< 1 mm) transparent layer of glass.

The support could be naturally coloured: greenish, yellowish, brownish supports are found in Byzantine mosaics (see e.g. Fiori et al. 2004) or colourless, with an intentional addition of a decolourant. The threshold values for the intentional addition for the decolourisers are 0.5 wt% for manganese (Jackson 2005) and 0.2 wt% for antimony (Sayre 1963) and these confirm the exclusive use of the former for the SAC colourless tesserae and of the latter for the SSV set (with the exclusion of SSV20): all but one of the colourless transparent glass samples of the SSV set are decolourised with antimony, with negligible contents of Mn. Manganese as a decolouring agent was employed in only one tessera (SSV20) whose provenance is from residual layers, and hence not archaeologically associable to the others. The most interesting feature, distinguishing the decolorized glasses from the *sacellum* and the monastery is, therefore, the use of a different decolourant.

As regards the base constituents, several authors have identified features of antimony decolourised colourless glass[5]. In comparison with the data reported in those works, the contents of antimony, iron, and manganese are compatible with antimony decolourised glass. Foster and Jackson (2010) compare the composition of their late roman Sb decolorized glass SSV glass with that of the coeval Mn- decolorized glass. And found that, on average the Sb-bearing has higher Al_2O_3 and K_2O, lower MgO, and slightly lower CaO, with respect to the Mn-bearing glass. Even if in all our samples the absolute amount are somewhat different, the situation is very similar: SSV colourless samples show, on average higher alumina and potash, and lower magnesia, with respect to SAC Mn-decolorized samples (2.18 vs 2.02 Al_2O_3, 0.63 vs 0.50 K_2O, 0.61 vs 0.96 MgO, 7.31).

In comparison with the data reported in those works, the contents of antimony, iron, and manganese are compatible with antimony decolourised glass, but the relatively low number of colourless samples in the present SSV set and the high variability of the other oxides (eg. Na_2O, SiO_2 and CaO) does not make it possible to establish correspondence with the groups isolated by other authors.

When considering the samples from the *sacellum*, a good comparison can be made with the metal leaf tesserae from Saint Vitale (Fiori et al. 2004): manganese is the only decolourant employed in the 6th century metal leaf tesserae in which antimony is not detected or – at most – not intentionally added. Byzantine gold leaf tesserae from St. Prosdocimus (Padua) analysed by Silvestri

[5] Nenna et al. 1997; Foy et al. 2003; Picon, Vichy 2003; Jackson 2005; Paynter 2006; Silvestri et al. 2008.

et al. (2011) show a more articulated situation in which the co-presence of antimony and manganese in 6th century colourless mosaic glass is attributed to glass recycling. On the other hand, in the colourless tesserae from Sagalassos (Schibille et al. 2012) three samples from the Apollo Klarios temple late 5th-early 6th century AD) are decolourised with manganese, reflecting a typical feature of the Byzantine production to which also the sacellum tesserae could be, therefore, attributed. However, in the same work by Schibille and co-workers, one colorless tesserae from the Roman Baths 4th century with antimony, with contents of MnO and Sb_2O_3 closely comparable with the data from SSV15 to 19 is presented. The data from Sagalassos would confirm the generally accepted trend of a later use of manganese as a decolourant, making it possible that the colourless tesserae from the monastery excavations would be of Roman production. However, samples SSV15a, b and 19, do not belong to the typical "Roman" range of base constituents (fig. 5). Notwithstanding the possibility of reuse of Roman tesserae, a new and dedicated production of antimony decolourized tesserae cannot be excluded: Neri and Verità (2013), employing a method of gold leaf dating, confirm the use of antimony in newly made tesserae well beyond the recognised limit of the 4th century. This would not exclude the recycling of Sb-based Roman glass to newly produce the tesserae found in the area of the Saint Severus monastery.

Conclusions

Glass tesserae of different colours and degrees of opacity were analysed. They originated from different contexts of the archaeological site of Saint Severus (Classe): the area of the monastery, the construction of which started at the end of the 9th century; the floor of the *sacellum*, first nucleus of the monumental area, dated to the second half of the 4th century; and from a *pastiche* of mosaic floor fragments removed from the original floor of the Saint Severus Basilica dated to the 6th century.

The main objectives of the work, besides widening and deepening knowledge of mosaic glass production in the area of Classe, near Ravenna, were to use chemical data to try to distinguish between three possible different glass productions, for which historical and archaeological information is incomplete.

As regards the source of flux, the analysed tesserae are all of the natron type, characteristic of a pre-10th-11th century Mediterranean production. All the tesserae are produced with siliceous calcareous sand containing a feldspatic component and, on the basis of the discrimination of the sole vitrifying raw materials, they all belong to typical Roman and late antique production, resembling to the vast majority of the Byzantine mosaic glass tesserae, either within a very close distance (Ravenna) or in farer Italian and Mediterranean sites. Following the model of primary to secondary glass production (Freestone et al. 2000; Nenna et al. 2000), the origin of the sands appear to be identifiable in the Levantine region; in fact, all the three analysed sets split into the two well-known groups of "Roman" and Levantine I" type. The data relative to other accessory components support the hypothesis of two different productions for each set of samples.

Therefore, it is not possible to make a distinction on the basis of the main components; however, an attempt can be made to compare the tesserae by considering the different origin of colours and the presence of characteristic elements. The main difficulty is obviously due to the imprecise correspondence of nuances; nonetheless, a direct comparison can be made:

Turquoise: the turquoise tesserae have common characteristics in the three sets, only small variation in Pb and Sn contents are observed. This, together with the scarcity of data regarding this particular colour, allow to hypothesise a specialised production, possibly not geographically diffused and with a long time tradition. The light-blue opaque glasses present only in the SSV set show similar characteristics.

Green-light green: the contents of lead and tin in the two SAC (4th century) and CR (6th century) sets are almost negligible if compared to those in the SSV (9th-10th century) sample set, in which lead and tin are definitely higher. In particular, the lead and tin rich green tesserae definitely belong to a different production, almost certainly of later chronology due to the high levels of tin.

Blue: are present only in SAC and CR sample sets and show clear similarities.

Red: no red samples were found in the mosaic of the *sacellum* and the CR sample can definitely be considered as belonging to a completely different production respect to the same colour of the SSV set that, in turn, show the generally recognised features of its specialized production.

Colourless: the only possible comparison can be made between the colourless samples from the SAC ans SSV sets. In SAC samples the decolourant is typical of Byzantine colourless tesserae (gold

or silver leaf tesserae): i.e. manganese, while the SSV samples were decolourized with antimony.

From the above discussion, the hypothesis that the tesserae from the basilica of Saint Severus (6th century) were reused to decorate important rooms of the later monastery (for example the chapter house) can be discarded and the possibility of a dedicated glass production could be put forth, at least for some of the colours (green and colourless). Secondly, the controversial chronology (original 4th century or a 9th century remake) of the mosaic from the *sacellum* can be partially solved: the present results demonstrate that the tesserae employed in the realisation of the *sacellum* mosaic are different from those of the monastery which could reasonably have been employed in a remake. However, this is not a guarantee that older tesserae were not re-employed in the realisation of the mosaic.

Indeed, it must be born in mind that the two floor decorations are artistic artefacts in which early and more recent interventions cannot be excluded, especially considering how easily the tiny tesserae blocks can be detached and substituted.

Acknowledgements

The authors wish to thank Paola Perpignani (Fondazione RavennAntica) and Ada Foschini (Laboratorio del Restauro Ravenna) for making available the samples taken during Prof. Augenti's excavations from the floor mosaics of the *sacellum* and *Cripta Rasponi*, respectively.

References

Andreescu-Treadgold, I., Henderson, J., Roe, M., 2006. Glass from the mosaics on the West wall of Torcello Basilica, *Arte Medievale* 5: 2-140.

Arletti, R., Quartieri, S., Vezzalini, G., 2006. Glass mosaic tesserae from Pompeii: an archeometrical investigation, *Periodico di Mineralogia* 76, 25-38.

Arletti, R., Ciarallo, A., Quartieri, S., Sabatino, G., Vezzalini, G., 2006a. Archaeometrical analyses of game counters from Pompeii, in M. Maggetti, B. Messiga, *Geomaterial in cultural heritage*, (Special Publication Geological Society of London 257), London: Geological Society of London: 175-86.

Arletti, R., Fiori, C., Vandini, M., 2010. A study of glass tesserae from mosaics in the Monasteries of Daphni and Hosios Loukas (Greece), *Archaeometry* 52: 796-815.

Arletti, R. Bertoni, E., Vezzalini, G., Mengoli, D., 2011. Glass beads from Villanovian excavations in Bologna (Italy): an archaeometrical investigation, *European Journal of Mineralogy* 23: 959-968.

Augenti, A., 2006a. Ravenna e Classe: archeologia di due città tra la tarda Antichità e l'alto Medioevo, in A. Augenti (a cura di), *Le città italiane tra la tarda antichità e l'alto Medioevo (Atti del Convegno, Ravenna, 26-28 febbraio 2004)*, Firenze: All'Insegna del Giglio: 185-217.

Augenti, A., 2006b. Ravenna e Classe: il racconto di due città, tra storia e archeologia, in A. Augenti, C. Bertelli (a cura di), *Santi Banchieri Re. Ravenna e Classe nel VI secolo. San Severo e il tempio ritrovato*, Milano: Skira: 17-22.

Augenti, A., 2010. San Severo: archeologia di un complesso monumentale, in P. Racagni (a cura di), *La Basilica ritrovata. I restauri dei mosaici antichi di san Severo a Classe*, Bologna: Ante Quem: 21-37.

Augenti, A., 2011-2012. Nascita, sviluppo e morte di una città tardoantica. Dieci anni di ricerche a Classe, *RendPontAc* 84: 77-120.

Augenti, A., Bondi, M., Carra, M., Cirelli, E., Malaguti, C., Rizzi, M., 2006. Indagini archeologiche a Classe (scavi 2004): primi risultati sulle fasi di età alto-medievale e dati archeobotanici, in R. Francovich, M. Valenti (a cura di), *Atti del IV Congresso di Archeologia Medievale* (Scriptorium dell'Abbazia, Abbazia di San Galgano, Chiusdino-Siena, 26-30 settembre 2006), Firenze: All'Insegna del Giglio: 124-131.

Augenti, A., Begnozzi, I., Bondi, M., Cirelli, E., Ferreri, D., Scozzari, P., 2012. Il monastero di San Severo a Classe: i risultati delle campagne di scavo 2006-2011, in F. Redi, A. Forgione (a cura di), *Atti del VI Convegno SAMI (L'Aquila, 2012)*, Firenze: All'Insegna del Giglio: 238-245.

Barber, D.J., Freestone, I.C., Moulding, K., 2009. Ancient copper red glasses: investigation and analysis by micro-beam techniques, in A.J. Shortland, I.C. Freestone, T. Rehren (eds.), *From Mine to Microscope. Advanced Study in Ancient Technology*, Oxford: Oxbow Books: 115-127.

Bermond Montanari, G., 1966. Scavi e ricerche nella zona della basilica di S. Severo, *Bollettino Economico della Camera di Commercio di Ravenna* 21: 12-18.

Bermond Montanari, G., 1968. *La chiesa di San Severo nel territorio di Classe*, Bologna: Patron.

Brill, R.H., Cahill, N.D., 1988. A red opaque glass from Sardis and some thoughts on red opaques in general, *Journal of Glass Studies* 30: 16-27.

Cable, M., Smedley, J., 1987. The replication o fan opaque red glass from Nimrud, in M. Bimson, I.C. Freestone (eds.), *Early vitreous materials* (British Museum Occasional Paper 56), London: British Museum: 151-164.

Christie, N., 2006. La chiesa e i mausolei, in A. Augenti (a cura di), *La basilica e il monastero di San Severo a Classe. La storia, gli scavi*, Ravenna: Fondazione RavennAntica: 11-14.

Cirelli, E., 2014. La ridefinizione degli spazi urbani nelle città dell'Adriatico centrale tra la tarda Antichità e l'alto Medioevo, *Hortus Artium Medievalium* 20: 39-47.

Cirelli, E., Lo Mele, E, 2010. La cultura materiale di San Severo alla luce delle nuove scoperte archeologiche, in P. Racagni (a cura di), *La Basilica ritrovata. I restauri dei mosaici antichi di San Severo a Classe*, Bologna: Ante Quem: 39-53.

Cirelli, E., Tontini, S., 2010. Produzione vetraria a Classe nella tarda antichità, in M. Vandini (a cura di), *Riflessioni e trasparenze: diagnosi e conservazione di opere e manufatti vetrosi (Atti del Convegno AIAr)*, Bologna: Patron: 125-133.

Di Bella, M., Quartieri, S., Sabatino, G., Triscari, M., Santalucia, F., 2014. The glass mosaic tesserae of "Villa del Casale" (Piazza Armerina, Italy): a multi-technique archaeometric study, *Archaeological and Anthropological Science* 6: 345-362.

Donovan, J.J., Rivers, M.L., 1990. PRSUPR: a PC-based automation and analysis software package for wavelength dispersive electron-beam microanalysis, in J.R. Michael, P. Ingram (eds.), *Microbeam Analysis*, San Francisco: San Francisco Press: 66-68.

Ferreri, D., 2011. Spazi cimiteriali, pratiche funerarie e identità nella città di Classe, *Archeologia Medievale* 38: 59-74.

Fiori, C., 2011. Vetro musivo del VI secolo dagli scavi della Basilica di San Severo a Classe (Ravenna), *Rivista della Stazione Sperimentale del vetro* 1: 22-34.

Fiori, C., 2013. Mosaic tesserae from the basilica of San Severo and glass production in Classe, Ravenna, Italy, in C. Entwistle, L. James (eds.), *New Light on Old Glass: Recent Research on Byzantine Glass and Mosaics*, London: British Museum Press: 33-41.

Fiori, C., Vandini, M., Mazzotti, V., 2004. *I colori del vetro antico. Il vetro musivo bizantino*, Padova: Il Prato.

Foschini, A., 2010. Il restauro dei mosaici della Cripta Rasponi presso il Palazzo della Provincia di Ravenna, in P. Racagni (a cura di), *La Basilica ritrovata. I restauri dei mosaici antichi di San Severo a Classe, Ravenna*, Bologna: Ante Quem: 259-266.

Foster, H., Jackson, C.M., 2009. The composition of 'naturally coloured' late Roman vessel glass from Britain and the implications for models of glass production and supply, *Journal of Archaeological Science* 36: 189-204.

Foster, H., Jackson, C.M., 2010. The composition of late Romano-British colourless vessel glass: glass production and consumpition, *Journal of Archaeological Science* 37: 3068-3080.

Foy, D., Picon, M., Vichy, M., Thirion-Merle, V., 2003. Caractérisation des verres de la fin de l'Antiquité en Méditerranée occidentale: l'émergence de nouveaux courants commerciaux, in D. Foy, M.-D. Nenna (éds.), *Échanges et commerce du verre dans le monde antique (Actes du colloque de l'Association Française pour l'Archéologie du Verre)*, Montagnac: Éditions Monique Mergoil: 41-85.

Freestone, I.C., 1987. Composition and microstructure of early opaque red glass, in M. Bimson, I.C. Freestone (eds.), *Early vitreous materials* (British Museum Occasional Paper 56), London: British Museum: 173-191.

Freestone, I.C., Bimson, M., Buckton, D., 1988. Compositional categories of Byzantine glass tesserae, in *Annales du 11e Congrès de l'Association Internationale pour l'Histoire du Verre (Bâle, 29 août-3 septembre 1988)*, Amsterdam: Edition de l'Association Internationale pour l'Histoire du Verre: 271-279.

Freestone, I.C., Gorin Rosen, Y., Hughes, M.J., 2000. Primary glass from Israel and the new production of glass in the lata antiquity and the early Islamic period, in M.-D. Nenna (éd.), *La route du verre. Ateliers primaires et secondaires du second millénaire av. J.-C. au Moyen Âge* (Travaux de la Maison de l'Orient Méditerranéen 33), Lyon: Maison de l'Orient Méditerranéen-Jean Pouilloux: 65-84.

Freestone, I.C., Stapleton, C.P., Rigby, V., 2003. The production of red glass and enamel in the Late Iron Age, Roman and Byzantine periods, in C. Entwistle (ed.), *Through a Glass Brightly: Studies in Byzantine and Medieval Art and Archaeology presented to David Buckton*, Oxford: Oxbow Books: 142-154.

Freestone, I.C., Bronk, H., Stapleton, C.P., 2008. *Why are red glasses different?* (oral communication at The Composition of Byzantine Glass Mosaic Tesserae. Leverhulme International Network, Workshop, 8-13 June 2008), Venice-Ravenna.

Gliozzo, E., Santagostino Barbone, A., Turchiano, M., Memmi, I., Volpe, G., 2012. The coloured tesserae decorating the vaults of the Faragola balneum (Ascoli Satriano, Foggia, Southern Italy), *Archaeometry* 54: 311-331.

Henderson, J., 2000. *The science and archaeology of materials. An Investigation of Inorganic Materials*, London: Routledge.

Henderson, J., McLoughlin, S.D., McPhail, D. S., 2004. Radical changes in Islamic glass technology: evidence for conservatism and experimentation with new glass recipes from early and middle Islamic Raqqa, Syria, *Archaeometry* 46: 439-68.

Jackson, C.M., 2005. Making colourless glass in the Roman period, *Archaeometry* 47: 763-780.

Lahlil, S., Biron, I., Cotte, M., Susini, J., Menguy N., 2010. Synthesis of calcium antimonate nano-crystals by the 18th dynasty Egyptian glassmakers, *Applied Phisycs A* 98: 1-8.

Lilyquist, C., Brill, R.H., 1993. *Studies in Ancient Egyptian Glass*, New York: Metropolitan Museum of Art.

Nenna, M.-D., Vichy, M., Picon, M., 1997. L'atelier de verrier de Lyon, du Ier siècle après J.-C., et l'origine des verres 'romains', *Revue d'Archeometrie* 21: 81-87.

Nenna, M.-D (éd.), 2000. *La route du verre: ateliers primaires et secondaires du second millénaire av. J.-C. au Moyen Age* (Travaux de la Maison de l'Orient Méditerranéen 33), Lyon: Maison de l'Orient Méditerranéen-Jean Pouilloux.

Neri, E., Verità, M., 2013. Glass and metal analyses of gold leaf tesserae from 1st to 9th century mosaics. A contribution to technological and chronological knowledge, *Journal of Archaeological Science* 40: 4596-4606.

Paynter, S., 2006. Analyses of colorless Roman glass from Binchester, County Durham, *Journal of Archaeological Science* 33: 1037-1057.

Paynter, S., 2008. Experiments in the reconstruction of Roman wood-fired glassworking furnaces: waste products and their formation processes, *Journal of Glass Studies* 50: 271-290.

Paynter, S., Kearns, T. 2011. *West Clacton Reservoir, Great Bently, Essex: analysis of glass tesserae* (Research Department Report Series 44): Portsmouth: English Heritage.

Picon, M., Vichy, M., 2003. D'Orient en Occident: l'origine du verre à l'époque romaine et durant le haut Moyen Âge', in D. Foy, M.-D. Nenna (édd.), *Échanges et commerce du verre dans le monde antique* (Actes du colloque de l'Association Française pour l'Archéologie du Verre, Aix en Provence-Marseille, 2001), Montagnac: Éditions Monique Mergoil: 17-31.

Santagostino Barbone, A., Gliozzo, E., Turchiano, M., D'Acapito, F., Memmi, I., Volpe, G., 2008. The sectilia panels of Faragola (Ascoli Satriano, Southern Italy): a multi-analytical study of the red, orange and yellow glass slabs, *Archaeometry* 50: 451-473.

Sayre, E.V., 1963. The intentional use of antimony and manganese in ancient glasses, in F.R. Matson, G.E. Rindone (eds.), *Advances in Glass Technology*, *Part 2*, New York: Plenum press: 263-282.

Schibille, N., Degryse, P., Corremans, M., Specht, C.G., 2012. Chemical characterization of glass mosaic tesserae from sixth-century Sagalassos (south-west Turkey): chronology and production techniques, *Journal of Archaeological Science* 39: 1480-1492.

Shortland, A,J., 2002. The use of antimonate colorants in early Egyptian glass, *Archaeometry* 44: 517-530.

Shugar, A., 2000. Byzantine opaque red glass tesserae from Beit Shean, Israel, *Archaeometry* 42: 375-384.

Silvestri, A., Molin, G., Salviulo, G., 2008. The colorless glass of Iulia Felix, *Journal of Archaeological Science* 35: 331-341.

Silvestri, A., Tonietto, S., Molin, G., 2011. The paleo-Christian glass mosaic of St. Prosdocimus (Padova, Italy): archaeometric characterisation of "gold" tesserare, *Journal of Archaeological Science* 38: 3402-3414.

Silvestri, A., Tonietto, S., Molin, G., Guerriero, P., 2014. The palaeo-Christian glass mosaic of St.Prosdocimus (Padova, Italy): archaeometric characterisation of tesserae with copper- or tin-based opacifiers, *Journal of Archaeological Science* 42: 51-67.

Stapleton, C.P., Freestone, I.C., Bowman, G.E., 1999. Composition and origin of early medieval opaque red enamel from Britain and Ireland, *Journal of Archaeological Science* 26: 913-922.

Tite, M., Pradell, T., Shortland, A,J., 2008. Discovery, production and use of tin-based opacifiers in glasses, enamels and glazes from the late iron age onwards: a reassessment, *Archaeometry* 50: 67-84.

Tontini, S., 2006. Vetri e produzione vetraria a Classe (Ravenna) in età tardoantica e altomedievale, *Bulletin* 15: 45-53.

Turner, W.E.S., Rooksby, H.P., 1959. A study of opalising agents in ancient opal glasses throughout three thousand four hundred years, *Glastechnische Berichte 32K* 7: 17-28.

Uboldi, M., Verità, M., 2003. Scientific analyses of glasses from late antique and early medieval archaeological sites in Northern Italy, *Journal of Glass Studies* 45: 115-37.

Van der Werf, I., Mangone, A., Giannossa, L.C., Traini, A., Laviano, R., Coralini, A., Sabbatini, L., 2009. Archaeometric investigation of Roman tesserae from Herculaneum (Italy) by the combined use of complementary micro-destructive analytical techniques, *Journal of Archaeological Science* 36: 2625-2634.

Vandini, M., Fiori, C., Cametti, R., 2006. Classification and technology of Byzantine mosaic glass, *Annali di Chimica* 96: 587-599.

Verità, M., Renier, A., Zecchin, S., 2002. Chemical analyses of ancient glass findings ex-

cavated in the Venetian lagoon, *Journal of Cultural Heritage* 3: 26-267.

Verità, M., Santopadre, P., 2009. Mosaico absidale della basilica di Santa Cecilia a Roma. Studio delle tessere vitree, in D. Radeglia (a cura di), *Restauri a Santa Cecilia. 25 anni di interventi dell'Istituto Superiore per la Conservazione e il Restauro*, Firenze: Edifir: 263-272.

Verità, M., 2011. Tessere vitree del battistero Neoniano: tecniche e provenienza, in C. Muscolino, A. Ranaldi, C. Tedeschi (a cura di), *Il battistero Neoniano. Uno sguardo attraverso il restauro*, Ravenna: Longo editore: 73-87.